Revised Version

DESY 03-161
Edinburgh 2003/15
LU-ITP 2003/017
LTH 593

arXiv:hep-lat/0310028 v2 8 Jan 2004

DESY 03–161
Edinburgh 2003/15
LU-ITP 2003/017
LTH 593

Quark spectra and light hadron phenomenology from overlap fermions with improved gauge field action*

D. Galletly[a], M. Gürtler[b], R. Horsley[a], B. Joó[a], A.D. Kennedy[a], H. Perlt[c], B.J. Pendleton[a], P.E.L. Rakow[d], G. Schierholz[b,e], A. Schiller[f] and T. Streuer[b,g]

QCDSF – UKQCD Collaboration

[a]School of Physics, University of Edinburgh, Edinburgh EH9 3JZ, UK

[b]John von Neumann-Institut für Computing NIC, Deutsches Elektronen-Synchrotron DESY, 15738 Zeuthen, Germany

[c]Institut für Theoretische Physik, Universität Regensburg, 93040 Regensburg, Germany

[d]Theoretical Physics Division, Department of Mathematical Sciences, University of Liverpool, Liverpool L69 3BX, UK

[e]Deutsches Elektronen-Synchrotron DESY, 22603 Hamburg, Germany

[f]Institut für Theoretische Physik, Universität Leipzig, 04109 Leipzig, Germany

[g]Institut für Theoretische Physik, Freie Universität Berlin, 14196 Berlin, Germany

We present first results from a simulation of quenched overlap fermions with improved gauge field action. Among the quantities we study are the spectral properties of the overlap operator, the chiral condensate and topological charge, quark and hadron masses, and selected nucleon matrix elements. To make contact with continuum physics, we compute the renormalization constants of quark bilinear operators in perturbation theory and beyond.

1. INTRODUCTION

Lattice calculations at small quark masses, i.e. in the chiral regime, require actions with good chiral properties. Overlap fermions [1] have an exact chiral symmetry on the lattice [2] and thus are predestined for this task. A further advantage of overlap fermions is that they are automatically $O(a)$ improved [3].

The massive overlap operator is defined by

$$D = \left(1 - \frac{am_q}{2\rho}\right) D_N + m_q, \qquad (1)$$

$$D_N = \frac{\rho}{a}\left(1 + \frac{X}{\sqrt{X^\dagger X}}\right), X = D_W - \frac{\rho}{a}, \qquad (2)$$

where D_W is the Wilson-Dirac operator. We assume $r = 1$ throughout this paper. The operator D_N has $n_- + n_+$ exact zero modes, $D_N\psi_n = 0$, n_- (n_+) being the number of modes with negative (positive) chirality, $\gamma_5\psi_n = -\psi_n$ ($\gamma_5\psi_n = +\psi_n$). The index of D_N is thus given by $\nu = n_- - n_+$. The 'continuous' modes λ, $D_N\psi_\lambda = \lambda\psi_\lambda$, having $(\psi_\lambda^\dagger, \gamma_5\psi_\lambda) = 0$, come in complex conjugate pairs λ, λ^*.

To compute the 'sign function'

$$\mathrm{sgn}(X) = \frac{X}{\sqrt{X^\dagger X}} \equiv \gamma_5\,\mathrm{sgn}(H),\ H = \gamma_5 X, \qquad (3)$$

we use Zolotarev's optimal rational approxima-

*Talks presented by M. Gürtler, R. Horsley, H. Perlt and T. Streuer at Lattice 2003.

tion [4]. To improve the accuracy of the rational approximation, and to reduce the number of iterations in the inner inversion, we project out the $\sim$ 16 lowest eigenvalues of H. The approximation of the 'sign function' is done to better than $5 \cdot 10^{-7}$ in the interval $[0.1, 2.4]$. We use a multi-mass conjugate gradient solver in both the inner and outer inversions. For any given quark mass this allows to compute propagators for a whole set of higher quark masses at very little extra cost in CPU time. For the inner and outer inversions a stopping criterion of 10^{-6} and $5 \cdot 10^{-6}$, respectively, is employed.

It is important to use a good gauge field action, because the inversion time of the fermion matrix is greatly reduced for improved gauge field actions. We use the Lüscher-Weisz action [5]

$$\begin{aligned} S[U] \;=\; \frac{6}{g^2}\Big[& c_0 \sum_{\text{plaquette}} \frac{1}{3}\,\mathrm{Re\,Tr}\,(1 - U_{\text{plaquette}}) \\ & +\; c_1 \sum_{\text{rectangle}} \frac{1}{3}\,\mathrm{Re\,Tr}\,(1 - U_{\text{rectangle}}) \\ & +\; c_2 \sum_{\text{parallelogram}} \frac{1}{3}\,\mathrm{Re\,Tr}\,(1 - U_{\text{parallelogram}})\Big] \end{aligned} \tag{4}$$

with coefficients c_1, c_2 ($c_0 + 8c_1 + 8c_2 = 1$) taken from tadpole improved perturbation theory [6]. In Fig. 1 we compare the condition number of the Wilson and tadpole improved Lüscher-Weisz gauge field action. We see that the condition number is a factor of $\gtrsim$ 3 larger for the Wilson action. This is largely due to the fact that the Lüscher-Weisz action suppresses dislocations [7] and thus greatly reduces the number of (unphysical) zero modes. Topological studies using the Wilson gauge field action should be taken with caution.

The calculations are mainly done on the $16^3 32$ lattice at $\beta = (6/g^2)\, c_0 = 8.45$, where [6] $c_1 = -0.15486$ and $c_2 = -0.013407$. The corresponding lattice spacing is $a = 0.095$ fm if we use $r_0 = 0.5$ fm to set the scale. We have taken $\rho = 1.4$, which we have found to be the optimal choice. In addition, part of the calculations have been done on the $12^3 24$ lattice at $\beta = 8.1$ to test for scaling. The lattice spacing here is $a = 0.125$ fm [6]. Both lattices have the same physical volume V.

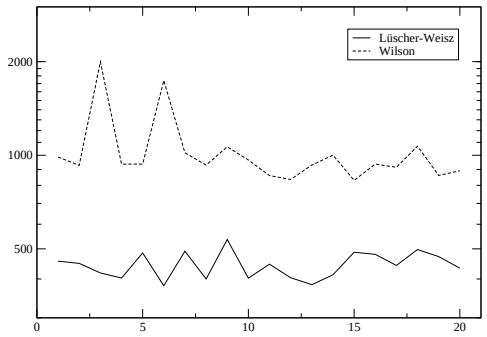

Figure 1. The condition number for the Wilson and tadpole improved Lüscher-Weisz gauge field action on the $16^3 32$ lattice at lattice spacing $a \approx 0.1$ fm for $\rho = 1.4$, as a function of configuration number.

2. SPECTRAL PROPERTIES

The eigenvalues of D_N lie on a circle around (ρ,0) with radius ρ in the complex plane. The improved operator $D_N^{\text{imp}} = (1 - a D_N/2\rho)^{-1} D_N$ [3] projects the eigenvalues of D_N stereographically onto the imaginary axis. The 'continuous' eigenvalues of D_N^{imp} come in pairs $\pm i\lambda$, while the zero modes are untouched.

We have computed the lowest $\approx$ 140 eigenvalues of D_N on both our lattices for $O(250)$ gauge field configurations each. We employed the Arnoldi algorithm as provided by the ARPACK package.

If one defines the topological charge density by $q(x) = (1/2)\,\mathrm{Tr}\,(\gamma_5 D_N(x,x))$ [8], the total charge Q is given by the index of D_N:

$$Q = \sum_x q(x) = n_- - n_+ . \tag{5}$$

Using this definition we have computed the topological susceptibility $\chi_{\text{top}} = \langle Q^2 \rangle / V$ and find

β	χ_{top}
8.10	$(195(5)\,\text{MeV})^4$
8.45	$(187(5)\,\text{MeV})^4$

(6)

The spectral density of the 'continuous' modes is

formally given by

$$\rho(\lambda) = \frac{1}{V}\Big\langle \sum_{\bar\lambda} \delta(\lambda - \bar\lambda)\Big\rangle, \qquad (7)$$

where the sum extends over the (nonzero) eigenvalues $\pm i\bar\lambda$ of $D_N^{\rm imp}$. In our case $0 < |\bar\lambda| \lesssim 800$ MeV. In practice one groups the eigenvalues into bins, whose size will depend on the statistics. In the infinite volume $\Sigma \equiv -\langle\bar\psi\psi\rangle = -\pi\rho(0)$. In the finite volume and for small eigenvalues the spectral density can be computed from the chiral low-energy effective theory. For $\lambda < E_T$, E_T being the Thouless energy $E_T \approx f_\pi^2/\Sigma\sqrt{V}$, the low-energy effective partition function is dominated by the zero momentum modes, and the zero-momentum approximation of the chiral low-energy effective theory is equivalent to chiral random matrix theory. In random matrix theory the microscopic spectral density in the sector of fixed topological charge Q,

$$\rho_S^{(Q)}(\Sigma V\lambda) \equiv \lim_{V\to\infty} \frac{1}{\Sigma}\,\rho(\lambda)\,\Big|_Q \qquad (8)$$

with $\Sigma V\lambda$ kept finite, is given by [9]

$$\rho_S^{(Q)}(x) = \frac{x}{2}\big(J_{|Q|}^2(x) - J_{|Q|+1}(x)J_{|Q|-1}(x)\big), \qquad (9)$$

where $J_n(x)$ are Bessel functions. Thus, for $\lambda < E_T$ the spectral density is given by

$$\rho(\lambda) = \Sigma\sum_Q w(Q)\,\rho_S^{(Q)}(\Sigma V\lambda), \qquad (10)$$

where $w(Q)$ is the weight of the sector of topological charge Q with $\sum_Q w(Q) = 1$. Taking $w(Q)$ from our 'measured' charge distributions, we then may obtain Σ by fitting (10) to our data. In Fig. 2 we show the data together with the fit for $\beta = 8.45$. We observe that random matrix theory describes the data well up to $\lambda \approx 150\,$MeV. For the (unrenormalized) chiral condensate we find $\Sigma = (242(8)\,\text{MeV})^3$ at $\beta = 8.1$ and $\Sigma = (249(9)\,\text{MeV})^3$ at $\beta = 8.45$. We will give renormalized values after we have computed the renormalization constants.

Random matrix theory predicts furthermore the distribution of the smallest nonzero eigenvalue in the sector of topological charge Q, which we call $\rho_{SE}^{(Q)}(\Sigma V\lambda)$. The first few expressions are [9]:

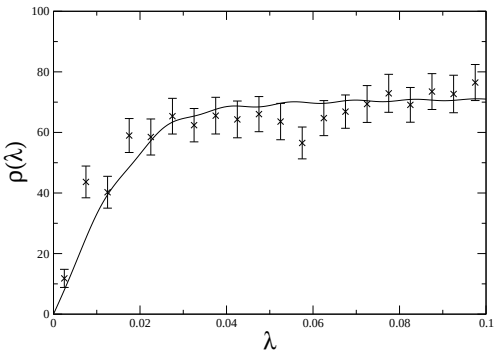

Figure 2. The spectral density $\rho(\lambda)$ at $\beta = 8.45$, together with a fit of random matrix theory to the data. Both ρ and λ are given in lattice units.

$$\begin{aligned}
\rho_{SE}^{(0)}(x) &= \frac{x}{2}\,e^{-x^2/2},\\
\rho_{SE}^{(1)}(x) &= \frac{x}{2}\,e^{-x^2/2} I_2(x), \qquad (11)\\
\rho_{SE}^{(2)}(x) &= \frac{x}{2}\,e^{-x^2/2}\big(I_2^2(x) - I_1(x)I_3(x)\big).
\end{aligned}$$

After having determined Σ from the spectral density of all eigenvalues, these formulae contain no free parameters anymore, and thus can be compared directly to our 'measured' distributions. In Fig. 3 we show our data together with the predictions of random matrix theory. We find good agreement.

3. RENORMALIZATION

To obtain physical results from lattice calculations of hadron matrix elements the underlying operators have to be renormalized. Let us denote the lattice regularized operators by $\mathcal{O}(a)$. We then define renormalized operators $\mathcal{O}^R(\mu)$ by introducing the renormalization constant $Z_{\mathcal{O}}(a\mu)$:

$$\mathcal{O}^R(\mu) = Z_{\mathcal{O}}(a\mu)\mathcal{O}(a). \qquad (12)$$

The renormalization constant $Z_{\mathcal{O}}(a\mu)$ is found by imposing the renormalization condition

$$\begin{aligned}
\Lambda_{\mathcal{O}}\big|_{p^2=\mu^2} &= Z_\psi(a\mu)Z_{\mathcal{O}}(a\mu)^{-1}\Lambda_{\mathcal{O}}^{\rm tree}\\
&+ \text{ other Dirac structures}, \qquad (13)
\end{aligned}$$

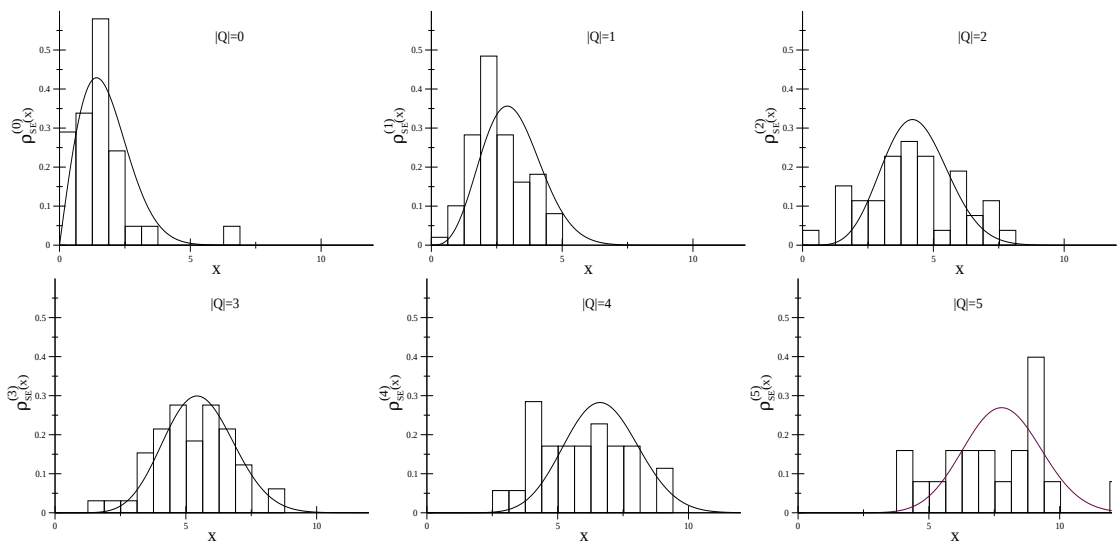

Figure 3. Distributions of the smallest nonzero eigenvalue $\rho_{SE}^{(Q)}(x)$ as a function of $x = \Sigma V \lambda$ for $|Q| = 0, \cdots, 5$ on the $16^3 32$ lattice at $\beta = 8.45$, together with the predictions of random matrix theory, in lattice units.

where Z_ψ is the wave function renormalization constant to be defined below and $\Lambda_{\mathcal{O}}$ is the forward (quark line) amputated Green function computed between off-shell quark states with 4-momentum p. We consider quark bilinear operators only. The renormalized operator $\mathcal{O}^R(\mu)$ is independent of the regularization scheme, but will depend on the external states and on the gauge. The operator matrix elements can be converted to more popular schemes like $\overline{MS}$ by means of continuum perturbation theory.

In the following we present first results of a perturbative calculation of renormalization constants for overlap fermions and improved gauge field action. So far results for overlap fermions are only known for the Wilson gauge field action [10,11]. The numbers given below hold for $c_1 = -0.15486$ and $c_2 = -0.013407$ (i.e. the improvement coefficients at $\beta = 8.45$), while we keep the (bare) coupling constant g arbitrary, which allows us to exchange it for a better expansion parameter.

The lattice Feynman rules for overlap fermions have been derived in [12,13]. The gluon propagator for improved gauge field action is known in four dimensions only [14,15]. A suitable form for dimensional regularization is

$$D_{\mu\nu}^{\mathrm{imp}} = D_{\mu\nu}^{\mathrm{Wilson}} + \Delta D_{\mu\nu}, \tag{14}$$

where

$$D_{\mu\nu}^{\mathrm{Wilson}} = \frac{1}{\hat{k}^2}\left(\delta_{\mu\nu} - \xi\,\frac{\hat{k}_\mu \hat{k}_\nu}{\hat{k}^2}\right), \tag{15}$$

is the standard Wilson propagator with $\hat{k}_\mu = (2/a)\sin(ak_\mu/2)$, and ξ specifies the gauge. The Landau gauge corresponds to $\xi = 1$, the Feynman gauge to $\xi = 0$. The six-link interaction terms are contained in $\Delta D_{\mu\nu} = D_{\mu\nu}^{\mathrm{Imp}} - D_{\mu\nu}^{\mathrm{Wilson}}$. While $D_{\mu\nu}^{\mathrm{Wilson}}$ leads to infrared divergent expressions, which have to be regularized, expressions involving $\Delta D_{\mu\nu}$ are infrared finite and thus can be computed in four dimensions. We may write

$$\begin{aligned}\Delta D_{\mu\nu} \;&=\; \delta_{\mu\nu}\sum_{n=0}^{4} D_n(\hat{k}, c_1, c_2)\,\hat{k}_\mu^{2n} \\ &+ \sum_{m,n=0}^{m+n=4} D_{m,n}(\hat{k}, c_1, c_2)\,\hat{k}_\mu^{2m+1}\,\hat{k}_\nu^{2n+1}.\end{aligned} \tag{16}$$

The coefficient functions D_n and $D_{m,n} = D_{n,m}$ are rational functions involving $\hat{k}$ and $c_{1,2}$. Explicit expressions are given in [16]. Both functions vanish in the limit $c_{1,2} \to 0$.

Self energy

The inverse of the massless quark propagator can be written in the form

$$S^{-1} = \mathrm{i}\,\not{p} - \Sigma^{\mathrm{lat}} \tag{17}$$

with

$$\Sigma^{\mathrm{lat}} = \frac{g^2\,C_F}{16\pi^2}\,\mathrm{i}\,\not{p}\,\Sigma_1(a^2p^2). \tag{18}$$

For the quark self energy Σ_1 we find

$$\begin{aligned}\Sigma_1(a^2p^2) &= (1-\xi)\,\ln(a^2p^2) \\ &+ 4.79201\,\xi + b_\Sigma\end{aligned} \tag{19}$$

with

$$b_\Sigma = -16.179. \tag{20}$$

From (19) we obtain the quark wave function renormalization constant

$$Z_\psi(a\mu) = 1 - \frac{g^2\,C_F}{16\pi^2}\,\Sigma_1(a^2\mu^2). \tag{21}$$

Local operators

Let us consider local operators

$$\mathcal{O}_X = \bar{\psi}\,\Gamma^X\psi \equiv X \tag{22}$$

now with

X	Γ^X
S	1
P	γ_5
V	γ_μ
A	$\gamma_\mu\gamma_5$
T	$\sigma_{\mu\nu}\gamma_5$

To find the renormalization constants we have to compute the amputated Green functions $\Lambda_{\mathcal{O}_X} \equiv \Lambda^X$. We obtain

$$\begin{aligned}\Lambda^{S,P} &= \{1,\gamma_5\} + \frac{g^2C_F}{16\pi^2}[-(4-\xi)\,\ln(a^2p^2) \\ &- 5.79201\xi + b_{S,P}]\,\{1,\gamma_5\},\end{aligned} \tag{23}$$

$$\begin{aligned}\Lambda_\mu^{V,A} &= \{\gamma_\mu,\gamma_\mu\gamma_5\} + \frac{g^2C_F}{16\pi^2}\Big\{[-(1-\xi)\,\ln(a^2p^2) \\ &- 4.79201\xi + b_{V,A}]\gamma_\mu \\ &- 2(1-\xi)\,\frac{p_\mu\,\not{p}}{p^2}\Big\}\,\{1,\gamma_5\},\end{aligned} \tag{24}$$

$$\begin{aligned}\Lambda^T_{\mu\nu} &= \sigma_{\mu\nu}\gamma_5 + \frac{g^2\,C_F}{16\pi^2}[\xi\,\ln(a^2p^2) \\ &- 3.79201\xi + b_T]\sigma_{\mu\nu}\gamma_5,\end{aligned} \tag{25}$$

where

$$\begin{aligned} b_{S,P} &= 10.512, \\ b_{V,A} &= 6.228, \\ b_T &= 3.900. \end{aligned} \tag{26}$$

Using (13) we then arrive at the renormalization constants

$$\begin{aligned} Z_{S,P} &= 1 - \frac{g^2C_F}{16\pi^2}[-6\ln(a\mu) - \xi + b_{S,P} + b_\Sigma], \\ Z_{V,A} &= 1 - \frac{g^2C_F}{16\pi^2}\,[b_{V,A} + b_\Sigma]\,, \\ Z_T &= 1 - \frac{g^2C_F}{16\pi^2}[2\ln(a\mu) + \xi + b_T + b_\Sigma]. \end{aligned} \tag{27}$$

In the $\overline{MS}$ scheme this gives

$$\begin{aligned} Z^{\overline{MS}}_{S,P} &= 1 - \frac{g^2C_F}{16\pi^2}\,[-6\ln(a\mu) - 5 + b_{S,P} + b_\Sigma]\,, \\ Z^{\overline{MS}}_{V,A} &= 1 - \frac{g^2C_F}{16\pi^2}\,[b_{V,A} + b_\Sigma]\,, \\ Z^{\overline{MS}}_T &= 1 - \frac{g^2C_F}{16\pi^2}\,[2\ln(a\mu) + 1 + b_T + b_\Sigma]\,. \end{aligned} \tag{28}$$

One-link operator

The one-link operator that will be of interest to us here is

$$\mathcal{O}_{\mu\nu} = \frac{\mathrm{i}}{2}\bar{\psi}\gamma_\mu\,\overleftrightarrow{D}_\nu\,\psi \;-\; \text{Traces}. \tag{29}$$

Two different irreducible representations of $\mathcal{O}_{\mu\nu}$ under the hypercubic group have been considered in the literature [17]:

$$\begin{aligned} \mathcal{O}_a &= \mathcal{O}_{\{14\}}, \\ \mathcal{O}_b &= \mathcal{O}_{44} - \frac{1}{3}\sum_{i=1}^{3}\mathcal{O}_{ii}, \end{aligned} \tag{30}$$

where $\{\cdots\}$ denotes symmetrization of the indices. Because of space limitations we will not give the Green functions here but only state the final results. For the renormalization constants of the operators $\mathcal{O}_{a,b}$ we obtain in the $\overline{MS}$ scheme

$$Z_{a,b}^{\overline{MS}} = 1 - \frac{g^2 C_F}{16\pi^2}\Big[\frac{16}{3}\ln(a\mu) + b_{a,b} + \frac{40}{9} + b_\Sigma\Big] \quad (31)$$

with

$$\begin{aligned} b_a &= -6.516, \\ b_b &= -5.617. \end{aligned} \quad (32)$$

Improvement

Lattice perturbation theory is known to converge badly due to the appearance of (gluon) tadpole diagrams, which are lattice artifacts and which make the bare coupling g into a poor expansion parameter. It was proposed [18] that the perturbative series should be rearranged in order to get rid of the tadpole contributions. We have made use of this observation already in tuning the coefficients of the Lüscher-Weisz action (4). For the renormalization constants this rearrangement is done in [16], following a method similar to that in [19]. Writing

$$Z_{\mathcal{O}} = 1 - \frac{C_F\, g^2}{16\pi^2}\tilde{B}_{\mathcal{O}}, \quad (33)$$

we arrive at the tadpole improved result

$$\begin{aligned} Z_{\mathcal{O}}^{TI} &= \frac{\rho\, u_0^{1-n_D}}{\rho - 4 + 4u_0}\Big\{1 - \frac{C_F\, g^2}{16\pi^2\, u_0^4}\Big[\tilde{B}_{\mathcal{O}} \\ &- \Big(1 - \frac{4}{\rho} - n_D\Big)k_u\Big]\Big\}, \end{aligned} \quad (34)$$

where

$$u_0 = \Big\langle \frac{1}{3}\mathrm{Tr}\, U_{\mathrm{plaquette}}\Big\rangle^{\frac{1}{4}}, \quad (35)$$

n_D is the number of covariant derivatives and [20] $k_u = 0.7325\,\pi^2$. The difference to the Wilson gauge field action is that $(1-n_D)\pi^2$ now has to be replaced by $(1-4/\rho-n_D)k_u$, and there is an additional prefactor of $\rho/(\rho-4-4u_0)$. At our value of β (i.e. $g^2 = 1.6658$) we find $u_0^4 = 0.65176$.

Alternatively, for the local operators (with $n_D = 0$) one may improve the perturbative result by writing [21]

$$Z_{\mathcal{O}}^{VI} = Z_V^{\mathrm{nonpert}}\Big[1 - \frac{C_F\, g^2}{16\pi^2}(\tilde{B}_{\mathcal{O}} - \tilde{B}_V)\Big], \quad (36)$$

where Z_V^{nonpert} is the nonperturbatively determined renormalization constant of the local vector current and Z_V^{pert} the perturbatively computed one. A similar procedure can be envisaged for the one- and higher-link operators. In that case Z_V^{nonpert} will have to be replaced by the appropriate nonperturbatively determined renormalization constant of the one- and higher-link operator, respectively.

In Table 1 we compare the results of the various improvement schemes with the perturbative result. For Z_V^{nonpert} we have taken the nonperturbative result $Z_A = 1.416$ derived below (eq. (48)).

$\mathcal{O}$	$Z_{\mathcal{O}}$	$Z_{\mathcal{O}}^{TI}$	$Z_{\mathcal{O}}^{VI}$
S, P	1.150	1.190	1.430
V, A	1.140	1.171	1.416
T	1.159	1.207	1.443
$\mathcal{O}_a$	1.257	1.335	-
$\mathcal{O}_b$	1.244	1.308	-

Table 1
Comparison of renormalization constants at the scale $a\mu = 1$ for $\beta = 8.45$ and $Z_V^{\mathrm{nonpert}} = 1.416$ in the $\overline{MS}$ scheme.

4. CHIRAL CONDENSATE

Knowing Z_S, we can now compute the renormalized chiral condensate

$$\langle\bar{\psi}\psi\rangle^R(\mu) = -Z_S(a\mu)\,\Sigma. \quad (37)$$

It is traditional to quote numbers for $\mu = 2$ GeV. In the $\overline{MS}$ scheme we obtain $Z_S^{TI}(2\,\mathrm{GeV}) = 1.253$

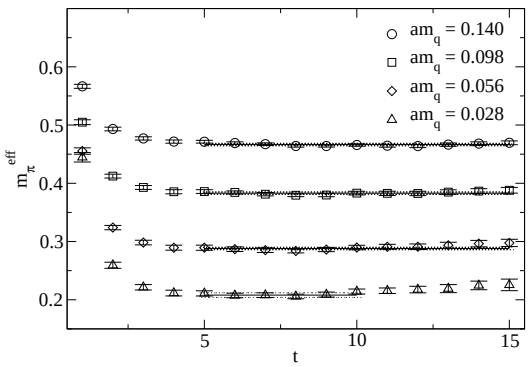

Figure 4. Effective pion masses for our four different quark masses from $\langle A_4(t)A_4(0)\rangle$.

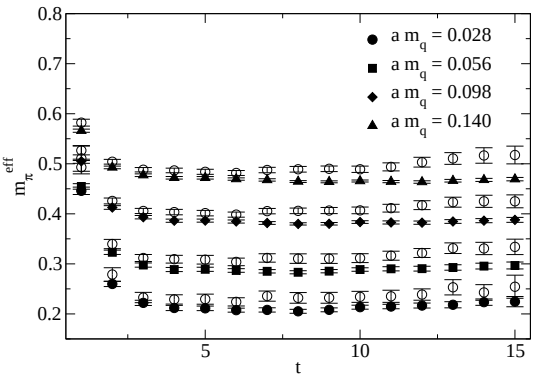

Figure 5. Effective pion masses from $\langle A_4(t)A_4(0)\rangle$ before (solid symbols) and after (open symbols) removal of zero modes from the quark propagators.

at $\beta = 8.1$ and $Z_S^{TI}(2\,\mathrm{GeV}) = 1.184$ at $\beta = 8.45$. This gives

β	$\langle\bar\psi\psi\rangle^{\overline{MS}}(2\,\mathrm{GeV})$
8.10	$(261(9)\,\mathrm{MeV})^3$
8.45	$(263(9)\,\mathrm{MeV})^3$

(38)

We find good agreement with scaling.

At $\beta = 8.45$ we have $Z_S^{VI}(2\,\mathrm{GeV}) = 1.426$. Using this value for the renormalization constant we obtain $\langle\bar\psi\psi\rangle^{\overline{MS}}(2\,\mathrm{GeV}) = (280(10)\,\mathrm{MeV})^3$.

5. QUARK AND HADRON MASSES

The results presented in this and the next Section refer to the $16^3 32$ lattice at $\beta = 8.45$. The calculations are done for four different quark masses, $am_q = 0.028, 0.056, 0.098$ and 0.140 (corresponding to $a\mu \equiv am_q/2\rho = 0.01, 0.02, 0.035$ and 0.05.) To increase the overlap of meson and baryon operators with the ground state wave function we use smeared sources [22] with $\kappa_s = 0.21$ and $N_s = 50$. The calculations of two-point functions are based on $O(100)$ configurations. The code has partly been written in SZIN [23], which has the advantage of being flexible and machine independent.

Pion mass

We compute the pion mass from various correlation functions: $\langle P(t)P(0)\rangle$, $\langle A_4(t)P(0)\rangle$ and $\langle A_4(t)A_4(0)\rangle$, where P is the pseudoscalar density and A_μ the axial vector current. In Fig. 4 we show the effective mass plot of $\langle A_4(t)A_4(0)\rangle$ for our four quark masses. This correlation function is least affected by finite size corrections induced by zero mode contributions [24,25]. The resulting pion masses are given in Table 2. Our lightest pion mass is $\approx 400\,\mathrm{MeV}$, which is compatible with quenched Wilson fermion calculations.

The correlation functions $\langle P(t)P(0)\rangle$ and $\langle A_4(t)P(0)\rangle$ give compatible results, albeit with larger error bars. If one explicitly removes the zero mode contributions from the quark propagators one arrives at the result shown in Fig. 5. It appears that the pion mass obtained from $\langle A_4(t)A_4(0)\rangle$ increases by $\approx$ 10% (5%) at the

am_q	am_π	m_π [MeV]
0.028	0.211(3)	439(6)
0.056	0.288(2)	599(4)
0.098	0.383(2)	797(4)
0.140	0.466(2)	969(4)

Table 2
Pion masses from $\langle A_4(t)A_4(0)\rangle$. We have used $a = 0.095$ fm to convert the lattice numbers to physical units.

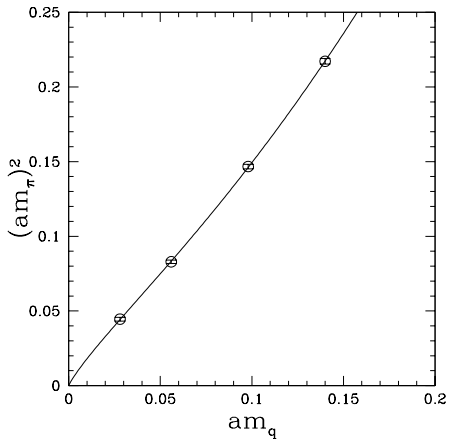

Figure 6. The pion mass $(am_\pi)^2$ as a function of am_q, together with the fit.

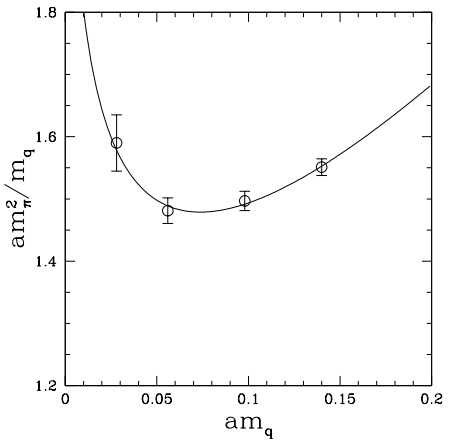

Figure 7. The ratio am_π^2/m_q as a function of am_q, together with the fit.

lowest (highest) quark mass. Whether this is a valid procedure to reduce finite size effects is not clear to us, because it involves a nonlocal step [26]. But it should be taken as a warning that finite size effects might still be large.

In Fig. 6 we plot m_π^2 against m_q, and in Fig. 7 we show the deviation of m_π^2 from linearity. Quenched chiral perturbation theory predicts, in the infinite volume,

$$m_\pi^2 = Am_q\big(1-\delta[\ln(Am_q/\Lambda_\chi^2)+1]\big)+O(m_q^2). \quad (39)$$

We fit our data by

$$m_\pi^2 = Am_q + Bm_q \ln m_q + Cm_q^2. \quad (40)$$

The result of the fit is shown by the curves in Figs. 6 and 7. Using $\Lambda_\chi = 4\pi f_\pi$ ($f_\pi = 93$ MeV), we derive $\delta = 0.26(9)$. This number agrees, within error bars, with what one would expect. However, before one can draw any conlusions, a careful study of finite size effects must be performed.

Quark masses

We determine the bare light and strange quark masses, $m_\ell = (m_u + m_d)/2$ and m_s, from the physical pion and kaon masses [27,28]:

$$m^2_{\pi\,\mathrm{phys}} = A\,m_\ell + B\,m_\ell \ln m_\ell + C\,m_\ell^2, \quad (41)$$

$$m^2_{K\,\mathrm{phys}} = A\,(m_\ell+m_s)/2 + B\,(m_\ell+m_s)/2 \times \Big(\frac{m_s \ln m_s - m_\ell \ln m_\ell}{m_s - m_\ell} - 1\Big) + C\,[(m_\ell+m_s)/2]^2. \quad (42)$$

We find $am_\ell = 0.0020(3)$ and $am_s = 0.068(2)$. The renormalized quark mass is given by $m_q^R = Z_m(a\mu)\,m_q$ with $Z_m = 1/Z_S$. Using $Z_S^{TI}(2\,\mathrm{GeV}) = 1.184$ (and $a = 0.095$ fm), we obtain

$$m_\ell^{\overline{MS}}(2\,\mathrm{GeV}) = 3.5(3)\ \mathrm{MeV}, \quad (43)$$

$$m_s^{\overline{MS}}(2\,\mathrm{GeV}) = 119(4)\,\mathrm{MeV}. \quad (44)$$

If we use $Z_S^{VI}(2\,\mathrm{GeV}) = 1.426$ instead, the numbers reduce to

$$m_\ell^{\overline{MS}}(2\,\mathrm{GeV}) = 2.9(3)\,\mathrm{MeV}, \quad (45)$$

$$m_s^{\overline{MS}}(2\,\mathrm{GeV}) = 99(3)\ \mathrm{MeV}. \quad (46)$$

The light quark mass m_ℓ should not be taken too seriously, because it is strongly affected by chiral logarithms.

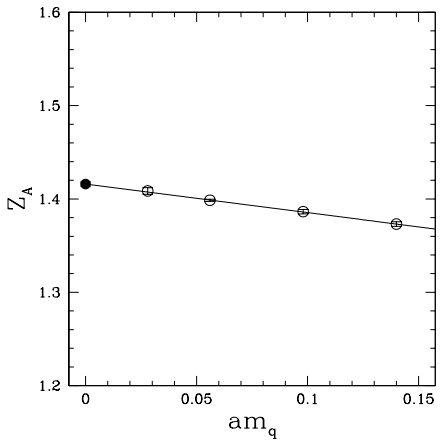

Figure 8. The renormalization constant Z_A as a function of am_q, together with the chiral extrapolation.

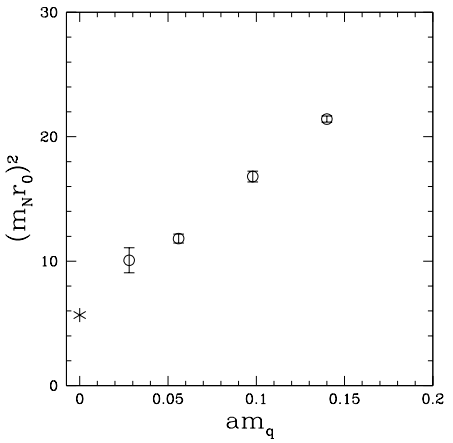

Figure 9. The nucleon mass $(m_N r_0)^2$ as function of am_q, together with the experimental result $(*)$, using $r_0/a = 5.26$.

Nonperturbative determination of Z_A

The renormalization constant Z_A can be computed nonperturbatively from the Ward identity (cf. [25])

$$Z_A = \lim_{t\to\infty} \frac{2m_q}{m_\pi} \frac{\langle P(t)P(0)\rangle}{\langle A_4(t)P(0)\rangle}. \qquad (47)$$

The result is plotted in Fig. 8. We see that Z_A depends only weakly on the quark mass. A linear extrapolation to the chiral limit gives

$$Z_A = 1.416(2). \qquad (48)$$

This number lies 20% above the tadpole improved perturbative result.

am_q	am_N	m_N [MeV]
0.028	0.60(3)	1250(60)
0.056	0.65(1)	1350(20)
0.098	0.775(10)	1612(20)
0.140	0.875(5)	1820(10)

Table 3
Nucleon masses. We have used $a = 0.095$ fm to convert the lattice numbers to physical units.

Nucleon mass

Our results for the nucleon mass are given in Table 3. In Fig. 9 we plot $(m_N r_0)^2$ against m_q. Except for the lowest mass, which currently is not very well determined, the data points lie on a straight line, which extrapolates surprisingly well to the experimental value.

6. NUCLEON MATRIX ELEMENTS

While hadron masses are determined from two-point correlation functions, nucleon matrix elements of quark bilinear operators $\mathcal{O}$,

$$\langle N|\mathcal{O}|N\rangle,\ \langle N|N\rangle = 2m_N, \qquad (49)$$

are derived from ratios of three-point to two-point functions,

$$R \equiv \frac{\langle N(t)\mathcal{O}(\tau)\bar{N}(0)\rangle}{\langle N(t)\bar{N}(0)\rangle} \simeq \frac{1}{2m_N}\langle N|\mathcal{O}|N\rangle, \qquad (50)$$

which for $t \gg \tau \gg 0$ are proportional to the desired matrix element, as shown on the r.h.s. of eq. (50). Here $N(t)$ is a suitable baryon operator. We consider nucleons of zero momentum only. This technique is by now standard. For details

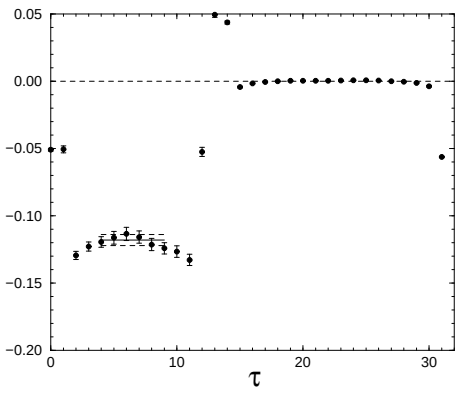

Figure 10. The ratio R plotted against the position τ of the operator $\mathcal{O}_b$ for $am_q = 0.14$. The source ($\bar{N}$) is placed at time slice $t = 0$, and the sink (N) at $t = 13$. From a plateau at $t \gg \tau \gg 0$ we can determine R.

and the numerical implementation the reader is referred to [22,29]. The calculation of three-point functions requires additional inversions and therefore is computationally expensive. The calculations in this Section are based on $O(50)$ configurations, so the results must be regarded as very preliminary.

While hadron masses are automatically $O(a)$ improved, operator matrix elements are generally not, except in the chiral limit. However, in distinction to improved Wilson fermions, improvement for overlap fermions is very simple and universal [3]:

$$\mathcal{O}^{\rm imp} = \left(1 - \frac{am_q}{2\rho}\right)^{-1} \mathcal{O}. \tag{51}$$

This a major advantage, as we do not have to compute matrix elements of higher dimensional operators, nor their associated improvement coefficients.

We shall consider two operators, the local vector current V_μ and the one-link operator $\mathcal{O}_b$. The nucleon matrix element of $\mathcal{O}_b$ yields the first moment of the unpolarized nucleon structure function. The results presented in this Section refer to improved, nonsinglet operators.

A typical ratio R is shown in Fig. 10 for the operator $\mathcal{O}_b$ from which we can find the bare nucleon matrix element.

Local vector current

Let us first look at the local vector current. Due to charge conservation

$$\langle N|V_\mu^R|N\rangle = Z_V \langle N|V_\mu|N\rangle = 2m_N\,, \tag{52}$$

which may be used to compute Z_V [30]. We expect $Z_V = Z_A$, and the idea is to test this hypothesis. In Fig. 11 we plot Z^V against am_q. We compare this result with Z_A computed from eq. (47) in Section 5. We see that Z_V approaches Z_A in the chiral limit, while at our largest quark mass the numbers differ by a few percent. Though the operators are $O(a)$ improved, discretization errors $\sim (am_\pi)^2$ are still possible, which might explain the small slope. A linear extrapolation to the chiral limit gives

$$Z_V = 1.426(7). \tag{53}$$

First moment of the structure function

Let us now turn to the operator $\mathcal{O}_b$. The nucleon matrix element of the operator $\mathcal{O}_a$ is much harder to compute, as it requires a nonzero nucleon momentum. The matrix element of the renormalized operator $\mathcal{O}_b$ gives [22]

$$\begin{aligned} \langle N|\mathcal{O}_b^R|N\rangle &= Z_b \langle N|\mathcal{O}_b|N\rangle \\ &= -2m_N^2 \langle x\rangle. \end{aligned} \tag{54}$$

For the tadpole improved renormalization constant in the $\overline{MS}$ scheme we find $Z_b^{\overline{MS}}(2\,\mathrm{GeV}) = 1.314$. In Fig. 12 we show the first moment of the nonsinglet nucleon structure function $\langle x\rangle$ in the $\overline{MS}$ scheme at $\mu = 2\,\mathrm{GeV}$. The numbers are in surprisingly good agreement with the experimental value. No nonanalytic behavior is needed to reconcile experimental and theoretical results. Previous calculations using Wilson fermions gave much larger values.

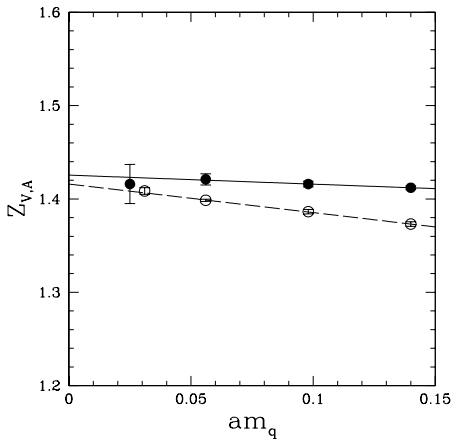

Figure 11. The renormalization constant Z_V from this calculation (solid symbols) compared with Z_A from Section 5 (open symbols) as a function of am_q, together with linear extrapolations to the chiral limit. The symbols at the lowest quark mass are displaced by a small amount so that they do not overlap.

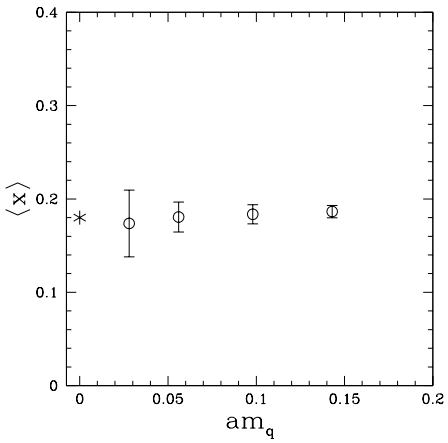

Figure 12. The first moment of the nucleon structure function $\langle x \rangle$ at $\mu = 2$ GeV as a function of am_q. Also shown is the phenomenological value $(*)$.

7. SUMMARY

Overlap fermions have many advantages over Wilson and staggered fermions. They provide an implementation of lattice fermions with exact chiral symmetry, even at finite lattice spacing. In addition, they are automatically $O(a)$ improved, and the task of operator renormalization is greatly reduced.

Calculations with overlap fermions on fine grained, phenomenologically relevant lattices are progressing rapidly. They are computationally costly, but by using an improved gauge field action and projecting out the lowest lying eigenvalues the condition number can be substantially reduced. We have tested the predictions of random matrix theory and find good agreement with the unfolded distributions of the smallest eigenvalue in topological sectors up to $|Q| = 5$. The renormalization constants of local and one-link operators have been computed perturbatively for the tadpole improved Lüscher-Weisz gauge field action. The one-loop corrections turn out to be relatively large, and in most cases significantly larger than in the improved Wilson fermion case [19], which calls for a nonperturbative determination. As a first step, we have computed Z_A and Z_V nonperturbatively. We find that Z_A and Z_V agree in the chiral limit, as expected. The nonperturbative numbers turn out to lie 20% higher than the tadpole improved perturbative values (at $a = 0.095$ fm). On the phenomenological side we have computed the topological susceptibility and the chiral condensate from the spectrum of low-lying eigenvalues. The topological susceptibility is found to be in good agreement with the Witten-Veneziano formula

$$m_{\eta'}^2 = \frac{2N_f}{f_\pi^2}\chi_{\rm top}, \qquad (55)$$

giving $m_{\eta'} = 920(50)$ MeV. We employed random matrix theory to derive the chiral condensate in the infinite volume. We went on to compute the pion, nucleon and quark masses. We find some signal for chiral logarithms. Both r_0/a [6], using $r_0 = 0.5$ fm, and the nucleon mass give compatible values for the lattice spacing. Our lowest pion mass so far is $m_\pi \approx 400$ MeV. There is quite a big uncertainty in the strange quark mass due to an

uncertainty in Z_m. Finally, we were able to compute the first moment of the nucleon structure function. Good agreement with the experimental value has been found.

ACKNOWLEDGEMENTS

The numerical calculations have been performed at NIC Jülich, ZIB Berlin and NeSC Edinburgh (IBM Regatta), NIC Zeuthen and Southampton (PC Cluster), and HPCF Cranfield (SunFire). We thank these institutions for support. This work is supported by the European Community's Human Potential Program under contract HPRN-CT-2000-00145 Hadrons/Lattice QCD and by DFG under contract FOR 465 (Forschergruppe Gitter-Hadronen-Phänomenologie).

REFERENCES

1. H. Neuberger, Phys. Lett. B417 (1998) 141; *ibid.* B427 (1998) 353.
2. M. Lüscher, Phys. Lett. B428 (1998) 342.
3. S. Capitani, M. Göckeler, R. Horsley, P.E.L. Rakow and G. Schierholz, Phys. Lett. B468 (1999) 150.
4. J. van den Eshof, A. Frommer, T. Lippert, K. Schilling and H.A. van der Vorst, Nucl. Phys. (Proc. Suppl.) 106 (2002) 1070.
5. M. Lüscher and P. Weisz, Commun. Math. Phys. 97 (1985) 59.
6. C. Gattringer, R. Hoffmann and S. Schaefer, Phys. Rev. D65 (2002) 094503.
7. M. Göckeler, A.S. Kronfeld, M.L. Laursen, G. Schierholz and U.-J. Wiese, Phys. Lett. B233 (1989) 192.
8. F. Niedermayer, Nucl. Phys. (Proc. Suppl.) 73 (1999) 105.
9. T. Wilke, T. Guhr and T. Wettig, Phys. Rev. D57 (1998) 6486.
10. C. Alexandrou, E. Follana, H. Panagopoulos and E. Vicari, Nucl. Phys. B580 (2000) 394.
11. S. Capitani, Nucl. Phys. B592 (2001) 183.
12. Y. Kikukawa and A. Yamada, Phys. Lett. B448 (1999) 265.
13. M. Ishibashi, Y. Kikukawa, T. Noguchi and A. Yamada, Nucl. Phys. B576 (2000) 501.
14. P. Weisz, Nucl. Phys. B212 (1983) 1.
15. Y. Iwasaki, Tsukuba preprint UTHEP-118 (1983).
16. R. Horsley, H. Perlt, P.E.L. Rakow, G. Schierholz and A. Schiller, in preparation.
17. M. Göckeler, R. Horsley, E.-M. Ilgenfritz, H. Perlt, P. Rakow, G. Schierholz and A. Schiller, Nucl. Phys. B472 (1996) 309.
18. G.P. Lepage and P.B. Mackenzie, Phys. Rev. D48 (1993) 2250.
19. S. Capitani, M. Göckeler, R. Horsley, H. Perlt, P.E.L. Rakow, G. Schierholz and A. Schiller, Nucl. Phys. B593 (2001) 183.
20. M.G. Alford, W. Dimm, G.P. Lepage, G. Hockney and P.B. Mackenzie, Phys. Lett. B361 (1995) 87.
21. A.S. Kronfeld, these proceedings.
22. M. Göckeler, R. Horsley, E.-M. Ilgenfritz, H. Perlt, P. Rakow, G. Schierholz and A. Schiller, Phys. Rev. D53 (1996) 2317.
23. See: `www.jlab.org/~edwards/szin/`.
24. T. Blum, P. Chen, N. Christ, C. Cristian, C. Dawson, G. Fleming, A. Kaehler, X. Liao, G. Liu, C. Malureanu, R. Mawhinney, S. Ohta, G. Siegert, A. Soni, C. Sui, P. Vranas, M. Wingate, L. Wu and Y. Zhestkov, `hep-lat/0007038`.
25. S.J. Dong, T. Draper, I. Horváth, F.X. Lee, K.F. Liu and J.B. Zhang, Phys. Rev. D65 (2002) 054507.
26. C. Gattringer, M. Göckeler, P. Hasenfratz, S. Hauswirth, K. Holland, T. Jörg, K.J. Juge, C.B. Lang, F. Niedermayer, P.E.L. Rakow, S. Schaefer and A. Schäfer, `hep-lat/0307013`.
27. C. Bernard and M. Golterman, Phys. Rev. D46 (1992) 853.
28. T. Yoshié, Prog. Theor. Phys. 105 (2001) 37.
29. C. Best, M. Göckeler, R. Horsley, E.-M. Ilgenfritz, H. Perlt, P. Rakow, A. Schäfer, G. Schierholz, A. Schiller and S. Schramm, Phys. Rev. D56 (1997) 2743.
30. T. Bakeyev, M. Göckeler, R. Horsley, D. Pleiter, P.E.L. Rakow, G. Schierholz and H. Stüben, `hep-lat/0305014`.